CA1 Term Report of ME5106

Measurement and Analysis on the Building Noise Properties

Wei Huanxia, Zeng Zhengtao, Kong Deyu, Li Hao Tian

1. Introduction

This is a CA1 report of ME5106. In this report, we measured the noise properties around The Parc Condominium, including two different blockes as well as different floors.

To obtain the results with higher precision, we built the measurement system includes condeser microphone, audio interface, and digital audio workstation Studio One. The system was calibrated by iZotope Ozone. After that, the noise level and the frequency charateristis were analyzed in iZotope Insights.

Based on them, we analyzed the sound level and frequency near the Ayer Rajah Expressway from The Parc Condominium. We also compared between BLK01 and BLK11 of this condo, which are facing to the different roads. What's more, as the lower floor are covered with trees serving as sound barrier, we analyzed the effects of them to the noise in the in-door areas.

2. The Theory of voice

2.1 The theory of Loudness

When conducting experiments in an area to measure sound data, the most immediate information accessible to humans is often whether the environment is noisy or not. We rely on our ears to assess the suitability of the environment for human habitation. In this evaluative process, the most convincing parameter is typically loudness.

Loudness, in this context, refers to the perceived magnitude of sound as detected by human ears. This definition tends to be relatively objective. However, in engineering, we frequently utilize several other measurable attributes to characterize the sounds we encounter.

2.1.1 Sound Intensity

One such attribute is sound intensity, which quantifies the power of sound flow per unit area. Essentially, it involves calculating this parameter by dividing the total power emitted by a sound source by the area through which it propagates. Due to the logarithmic nature of human ear perception, sound intensity is typically expressed using logarithmic scales. The definition of Sound Intensity Level is as follows:

$$\mathrm{SIL} = 10\log_{10}\left(\frac{I}{I_{ref}}\right) \quad (1.1.1)$$

Here, I represents the actual density of power of sound(W/m^2), I_{ref} represents the reference sound power density($10^{-12}W/m^2$).

Due to the human ear's sensitivity to changes in sound intensity, where the smallest perceptible change occurs when the ratio of sound intensities changes by tenfold, we employ a multiplication coefficient of 10. This tenfold change in sound intensity level is termed one Bel. Therefore, the unit of sound intensity is the decibel (dB)[1].

2.1.2 Sound Power Level

Another attribute is Sound Power Level, which represents the magnitude of the total power radiated by a sound source. It is often denoted using SWL or PWL. This attribute is also quantified using logarithmic ratios:

$$SWL = 10\log_{10}\left(\frac{W}{W_{ref}}\right) \quad (1.1.2)$$

This attribute is frequently employed to analyze the total power of a sound source.

2.1.3 Sound Pressure Level

Sound pressure is defined as the root mean square value of the excess instantaneous pressure generated by sound waves at a certain point. It is frequently used to describe the magnitude of sound wave due to human ear's sensitivity to it, and it is easily measurable. Sound pressure level is also commonly represented logarithmically:

$$SPL = 20\log_{10}(\frac{P}{P_{ref}}) \quad (1.1.3)$$

Here, using 20 as the multiplication coefficient serves two mean purposes. One is to align an integer change in sound pressure level with the minimum change in sound pressure perceptible to the human ear. Another is to maintain consistency between the measurement of sound pressure level and sound intensity level.

2.2 Spectrum theory

During both simulation and experiments, the primary attribute we can directly measure is the sound pressure level. However, the data obtained from this measurement often lacks organization, making it difficult to extract useful insights for analyzing the environment. Therefore, we require methods to transform this disordered information into a more useful form. During the experiments of sound measurement the data we directly measure is typically in the time domain, representing the pressure level resulting from the combination of multiple sounds. The knowledge we can extract from this signal is quite limited. Therefore, it is essential to transform this signal into the frequency domain. During this process, Discrete Fourier Transform is of vital importance.

This Discrete Fourier Transform is the discrete version of a continuous Fourier Transform, it is suitable for signal with limited length. The discrete Fourier transform can convert a signal containing N sample points to N complex numbers, where each complex number represents the amplitude and phase of the signal at different frequencies.

The Fourier Transform pair for continuous signals can be written in the form[2][5].

$$X(f) = \int_{-\infty}^{\infty} x(t)e^{-i2\pi ft}\,dt \quad (1.2.1)$$

$$x(t) = \int_{-\infty}^{\infty} x(t)e^{i2\pi ft}\,df \quad (1.2.2)$$

For $-\infty < f < \infty, -\infty < \mathrm{t} < \infty$, and $\mathrm{i} = \sqrt{-1}$. Here, the uppercase $X(f)$ represents the frequency- domain function; the lowercase $x(t)$ is the time- domain function.

The analogous discrete Fourier transform pair that applies to sampled versions of these functions can be written as:

$$X(j) = \frac{1}{N}\sum_{k=0}^{N-1} x(k)e^{-i2\pi jk/N} \quad (1.2.3)$$

$$X(k) = \sum_{j=0}^{N-1} X(j)e^{i2\pi jk/N} \quad (1.2.4)$$

For j= 0, 1, …, N-1; k = 0, 1, …, N-1. Both $X(j)$ and $X(k)$ are complex series.

The discrete Fourier Transform can be efficiently calculated using the Fast Fourier Transform (FFT) algorithm [3], which makes it widely used in digital signal processing and spectrum analysis. This FFT algorithm decomposes DFT into smaller scale DFTs and recursively applies these smaller scale DFTs to achieve efficient computation. This decomposition process greatly reduces the computational complexity of DFT.

These algorithms are the basic methods to transform the signal from time domain to frequency domain.

2.3 Electric Frequency Theory

All the signal we can detect in the real world should first be transformed into electrical signals using different kinds of sensors. After a series of complex signal processing in the electrical signal, we have a spectrum that can reflect the information we need.

During the signal acquisition stage, to fully recover a signal, the sampling frequency must be at least a multiple of the highest frequency in the signal. This is because when the signal is sampled, if the sampling frequency is too low, the high- frequency components of the signal may be aliased by the low-frequency signal during the sampling process and become distorted, making it impossible to correctly reconstruct the original signal.

Here, according to the Nyquist Sampling Theorem [6], the highest frequency present in the original signal is defined as Nyquist Frequency, denoted as f_N . Consequently, the minimum required to accurately capture the signal is known as the Nyquist Sampling Frequency, denoted as f_{NS}. These two parameters are interrelated according to the following equation:

$$f_{NS} = 2f_N \quad (1.3.1)$$

If the sampling frequency does not obey this law, the restored signal will be distorted.

2.4 Theory of Insertion loss

Insertion loss is the definition which refers to the effect of acoustic materials or equipment used to reduce noise propagation or control sound propagation. Specifically, insertion loss refers to the degree to which sound energy is lost after passing through soundproofing materials or acoustic equipment.

Insertion loss is usually expressed in dB, representing the power loss of noise after passing through soundproofing materials or acoustic equipment. A higher insertion loss value represents a more effective sound insulation effect.

In the field of engineering acoustics, insertion loss is commonly used to evaluate the performance of acoustic equipment ,which is used to reduce the power of noise, such as soundproofing materials, soundproofing walls, soundproofing windows, soundproofing doors, etc. By measuring insertion loss, engineers can understand the effectiveness of these acoustic devices in reducing noise propagation and make adjustments and improvements as needed.

Insertion loss is commonly calculated using the formular below [4]:

$$Insertion\ Loss = 10\log_{10}\left(\frac{P_{in}}{P_{out}}\right) \quad (1.5.1)$$

Here, P_{in} represents the input sound power before propagates to soundproofing materials or acoustic equipment; P_{out} is the output sound power of sound passing through soundproofing materials or acoustic equipment.

3. Measurement System

3.1 Hardware

For the measurements, our group chose to use a combination of condenser microphones, audio interfaces, and digital audio workstation (DAW) in order to get a high degree of accuracy in loudness and frequency measurements. The device list is shown in the following table. It is also worth noting that, the total cost of the system is very low. The total system connection structure is shown in Figure 3.1.

Table 1. The device list for measurement.

Device name	Brand	Model	Version
Condeser Microphone	TakStar	PC-K200	N/A
Audio Interface	Behringer	UMC22	External Version
Computer	Lenovo	Y9000P	2023
Digital Audio Workstation	Presonus	Studio One Pro	V 6.5.2
Analysis Platform	iZotope	Ozone	11 Complete Bundle
Calibration Equalizer	FabFilter	Pro-Q 3 Linear	V2021
Analog Audio Cable	Choseal	XLR high-end cable	1.5 m

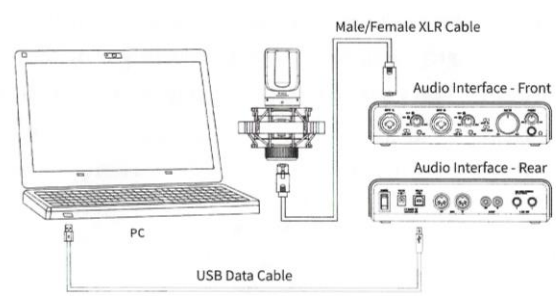

Figure 3.1. The system connection structure.

Condeser Microphone. A condenser microphone is essentially a capacitor that utilizes the principle of charging and discharging so that an ultra-thin metal or gold-plated plastic film acts as a vibrating membrane to sense sound pressure, collect the sound signal and then convert it into an electrical signal.

First, it will complete its initial charge buildup when energized (at which point the indicator light will gradually be illuminated). This means that the parallel plate capacitor starts charging. Once the charging is complete, the parallel plate capacitor has accumulated a charge, which is Q = external bias voltage value × diaphragm-backplane capacitance value. When the acoustic pressure on the diaphragm, the parallel plate capacitor of the two pole plate spacing d began to increase or decrease, diaphragm - back plate capacitance value C and the pole plate spacing d of the relationship between the formula is shown below.

$$C = \frac{\varepsilon_r S}{4\pi k d} \qquad (3.1)$$

As d decrease, C will increase. Then, when the charge is a constant between two planes, the voltage U will change, due to the following relationship.

$$C = \frac{Q}{U} \qquad (3.2)$$

Therefore, the output U is a function to C. when the C increases, the voltage becomes lower. Finally, we got the function between the sound pressure and output voltage U. (3.3)

Compared to moving coil microphones and electret microphones (commonly used in cell phones), condenser microphones have a very wide range of distance (due to its linear sound-voltage relationship) and flatter frequency response. Among other things, condenser microphones have a great advantage for frequencies below 100Hz and above 15kHz. Due to its principle of operation (which requires a charge between the electrodes), an external voltage needs to be added. This voltage will act as the DC component of the signal (known as the polarization voltage), while the actual sound signal will be converted to an AC signal. The two are superimposed to get the final test signal of the microphone sensor (not the complete microphone), which is the output. This signal is then amplified by an active circuit and the DC component is removed by a set of isolation capacitors and fed into the audio interface.

For the final output after physical signal processing, the DC component was remove, and the signal of sound (also a voltage signal via time) becomes the following.

$$V_{out} = U - \overline{U} = \left(\frac{V}{d_0}\right)\Delta d \qquad (3.4)$$

In which, the d_0 represents for the initial distance of capacitor, and V_{out} is the signal which will be send to audio interface then.

The most commonly used phantom power supplies are +12V, +24V, and +48V. we choose +48V to drive the condenser microphone. More specifications are shown in Table 2, and the frequency response curve provided by Takstar Laboratory is shown in Figure 3.2a.

Table 2. Detailed specifications of PC-K200 condeser microphone.

Specification	Value or Feature
Capsule	F16mm condenser
Polar Pattern	Cardioid (shown in Figure 3.2b)
Frequency Response	20 Hz - 20 kHz
Sensitivity	-36 dB ± 3 dB (0dB=1V/Pa @1kHz)
Output Impedance	200 Ω ± 30% (@1kHz)
Equivalent Noise Level	≤24 dBA due to IEC 581-5
Max SPL	130 dB (THD≤1% @1kHz)

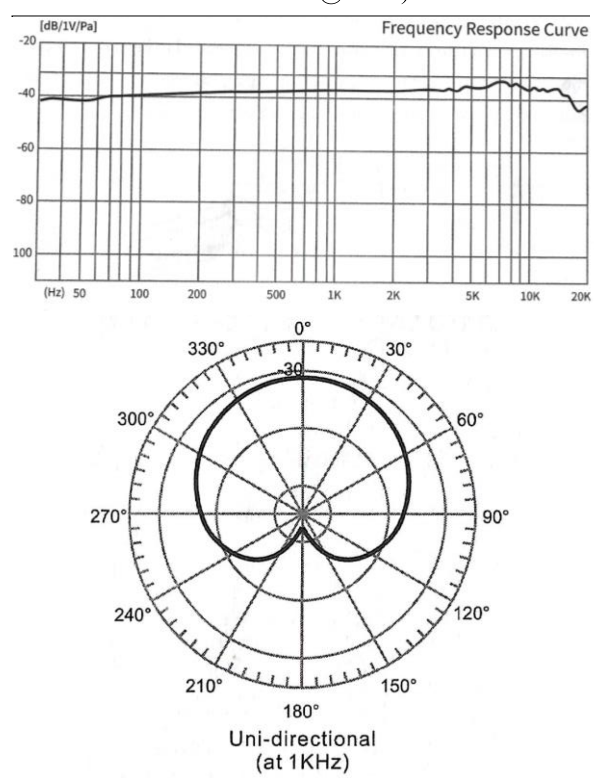

Figure 3.2. Specification of PC-K200. (a) the frequency response, and (b) the uni-directional feature as cardioid type.

As can be obtained from the table, the maximum response SPL is 130 dB, which proves that it works within the tolerance range. In addition, although most sources suggest that a non-polarized is supposed to be used in environmental acoustic measurements. However, since none of the measurements in this case were concerned with the acoustic information on the back side of the microphone (or the side close to the building and room), the cardioid type was used. Actually, the more important reason is that we don't own a non-polarized condenser microphone and would not like to buy one currently.

Audio interface. Audio interface, also known as analog-to-digital digital-to-analog converter (ADDA). For our measurements, only the AD function is used, namely convert the analog signal from condeser microphone to digital format, and then send it to DAW for real time, which is also known as sampling. For this process, the most important is the sampling rate, which means the sampling frequency via time, shown in Figure 3.3a. It is able to convert signals at higher frequencies (up to typically 96kHz or 192kHz, the latter commonly for top-level audio interfaces, which our hardware cannot support). Based on the Nyquist frequency theory, the limit of hearing for the human ear is 20kHz, so the sampling frequency (without considering interference effects such as comb filtering) is 40kHz. in electroacoustic engineering, the most common sampling rates are 44.1kHz and 48kHz. we chose 48kHz for our sampling process. on the other hand, the sample depth can be defined according to the length of the sampled bit data, shown in Figure 3.3b. We chose 24 bits as the sampling depth for our project, which is the highest sampling depth that can be achieved without using floating point recording. For the transfer of downstreamed digital signal, this interface comes with Audio Stream Input Output (ASIO) functions to obtain better recording performance with more stable connections. Actually, the audio interface serves as a data acquisition device (DAQ) in our measuring system.

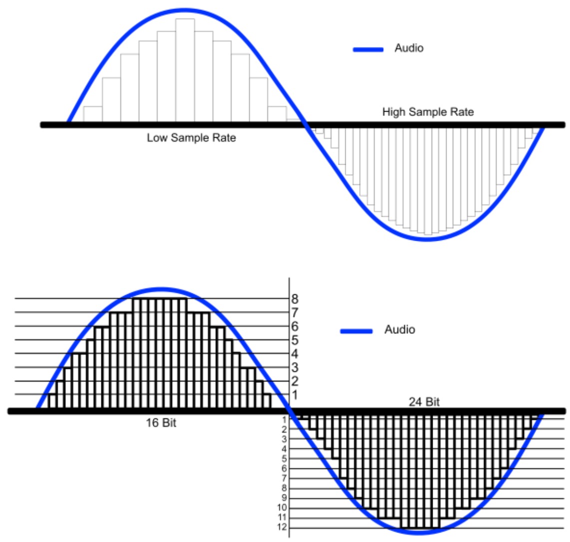

Figure 3.2. Sampling rate and bit depth.

3.2 Software

Digital Audio Workstation (DAW). DAW is a kind of integration platform for acoustic engineering. It provides a wide range of tools for recording, analysis, editing, time controlling, and reporting. Commonly used DAWs include protools, cubase, studio one, mixbus, nuendo, etc. As one of us has bought studio one only, therefore, we used studio one for measurement and part of the analysis.

Studio One is one of the most professional platforms among all DAWs, especially its support for Virtual Studio Technology Gen3 (VST3) , expanding its applications with a great number of plugins by many manufactories, one of them is iZotope Ozone, which was applied for analysis by us, and later introduced.

In our project, all the formats of the tracks are conFigureured to mono, as we did not use stereo microphone patterns for recording. For the hardware-software matrix mapping, the input of DAW is mapped to the XLR input of audio interface with phantom power. The total project in Studio One for measurement and analysis is shown in Figure 3.4. All of the tracks (including calibration track and the measurement tracks) are send to a buss track. Then, the signal will be corrected for frequency with Fabfilter Pro-Q3 as calibration equalizer, aiming to counteract the unbalanced frequency response of microphone and signal transmission process. After that, a Presonus dynamics processor is applied to calibrate the relationship between the digital audio signal and the physical sound level. Finally, the proper sound level as

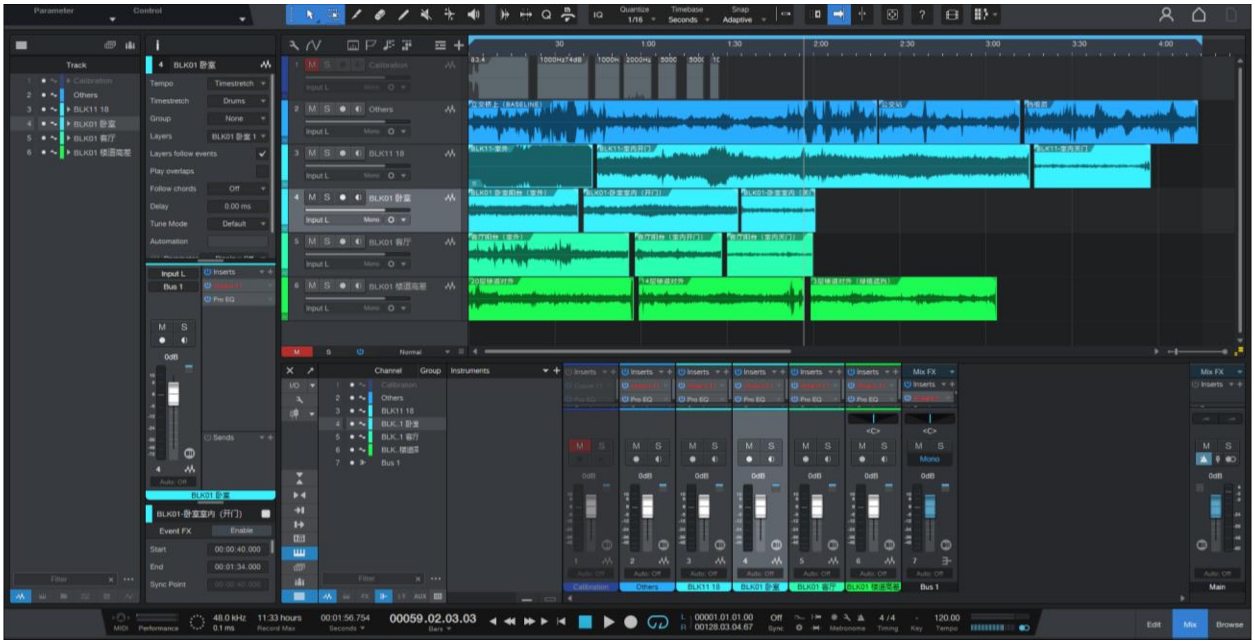

Figure 3.4. The conFigureurations and setups in the DAW for recording, calibration and analysis.

well as the frequency properties could be directly obtained at the downstream of the plugin slots of the buss track, where we inserted an audio analyser, provided by Ozone Insight.

Izotope Ozone. Izotope Ozone is a mastering toolkit for digital audio, providing multiple signal processing tools like dynamics, equalizer, sound meter, frequency meter, etc. Although it is originally designed for mastering engieering, these functions are also powerful for acoutics measurement, calibration, and analysis. In particular, conventional equalizers alter the original phase throughout their operation, causing them to introduce more unpredictable signal components, even obtain artifacts. The Ozone Equalizer offers a linear phase mode, based on Finite Impulse Response (FIR) filter algorithms, replacing the Infinite Impulse Response (IIR) filters used by tranditional equalizers.

Izotope Insight. Insight is a intelligent sound meter and analysis platform. It provides a range of methods for visualizing and analyzing audio in the time and frequency domains (or a combination of both). It will be used and described in more detail later in the analysis section.

3.3 Calibration

The calibration was conducted in Dynamics Laboratory at E1-2-3. First, we performed a loudness calibration. Along with the rest of the class students, we used the system to collect data from the sound source (a small circular speaker). The signal used in this step was white noise, namely full band noise. We then adjusted the attenuator and calibration data in the DAW, so that the data presented in the sound meter of the analysis buss track was always consistent with the standard equipment (a indutrial high-precision sound meter as reference from the lab).

Since the system has different amounts of attenuation for different frequencies (i.e., there is an unbalanced response curve), we also calibrated the frequencies. The calibration was done by comparing a sine wave pure tone generator, the original signal recorded in our lab, and the data from a calibration sound meter as a reference. Afterwards, we used an Izotope Ozone Equalizer (worked under the linear-phase mode) to correct the frequencies, resulting in measurements within 2dB of each octave in the range of 20Hz-20kHz.

3.4 Measurement

Based on the above tools, conFigureurations, and calibrations, the measurement process becomes very simple and the results are easy to read. In fact, all signal post-processing and analysis processes are done automatically in iZotope Insight and Presonus Sound Meter. More information about the measurements can be found in the later sections.

4. Results

4.1 Overview of sound experiment at locations close to the AYE

In order to explore the influencing factors of the measured noise levels, our group initiated the experiment by choosing three different locations for comparison. To start with the assignment, we selected the Ayer Rajah Expressway (AYE) at the intersection of Clementi Avenue 6 and West Coast Way as the source of the noise.[7] Figure 4.1 briefly provides an overview of the locations where noise testing was conducted along Clementi Avenue 6 and West Coast way at the AYE. We monitored the noise data on a pedestrian overpass as shown in Figure 4.2, designated as sound test location 1; at a bus station as shown in Figure 4.3, which is location 2; and behind a concrete wall as shown in Figure 4.4, which is location 3. We conducted sound tests in various locations, and enhanced the overall accuracy and reliability of the data collection, which could reduce the impact of random factors on individual measurements. Additionally, this method makes us easier to pinpoint noise sources, resulting in a straightforward method to find the sound propagation paths. To analyze the sound effects in different locations, the data presented in Figure 4.5, Figure 4.6, and Figure 4.7 will reveal the regions with distributed noise and those that are relatively quiet. These Figure 4.s also depict the noise energy levels at various frequencies (measured in decibels(dB). By comparing these Figure 4.s, we can evaluate the peak noise levels at different locations and determine whether these peaks occur within low-frequency or high-frequency zones.

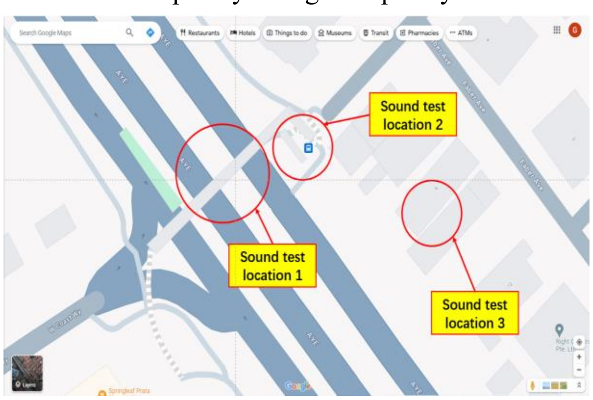

Figure 4.1. Locations of the sound test

Figure 4.2. On the Pedestrian Overpass

Figure 4.3. Bus station

Figure 4.4. Behind the concrete wall

4.1.1 Noise Results at locations close to the AYE

Table 1. Sound measurements along AYE

Measurement location: Along AYE	Max Sound Level/dB	Min Sound Level/dB	Ave Sound Level/dB
On the Pedestrian Overpass	81.6	50.4	67.5
Bus station	88.8	50.7	65.6
Behind the concrete wall	75.4	51.6	63.1

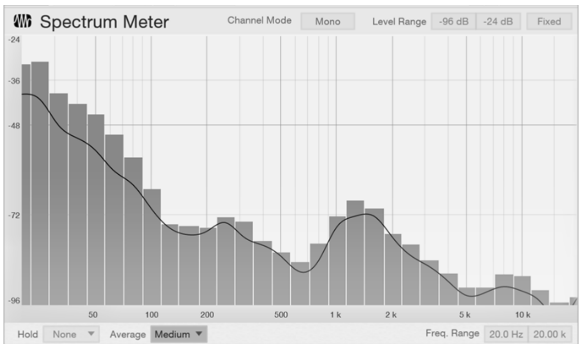

Figure 4.5. Spectrum of Pedestrian Overpass

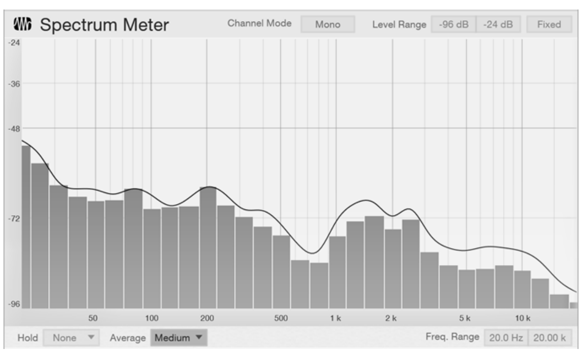

Figure 4.6. Spectrum of Bus Station

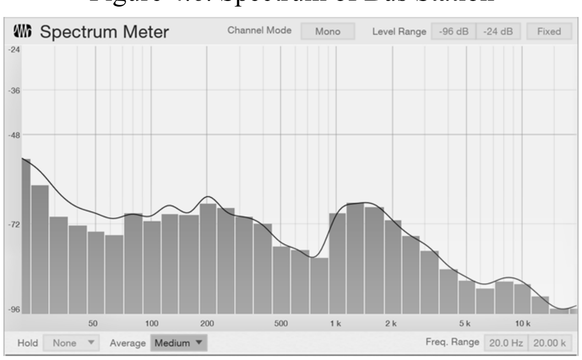

Figure 4.7. Spectrum of behind the concrete wall

4.1.2 Noise Results Comparison

The results of our measurements in this region are shown in Table 1. The overall sound level of the Pedestrian Overpass is the largest of the three. Due to the concrete wall, the sound level behind the wall is lower than at the bus station, which is located on the side of the road , despite the two measuring points being close to each other.

The results from Figure 4.5, 6 and 7 are collected from the spectrum meter, and the white line shows the data of noise level with respect to the frequency range. The noise level range in these graphs starts from -96dB to -24dB, and the frequency range starts from 20 Hz to 20k Hz. Compared to Figure 4.5, 6 and 7, there are some differences of noise level at the low frequency from approximately 20 Hz to 50 Hz. However, there are almost no differences in the high frequency zones where from 5k Hz all the way close to the 20k Hz. More importantly, Figure 4.5 is the spectrum of pedestrian overpass that has the highest peak noise level at the lower frequency range when compared to the spectrum of the bus station and behind the concrete wall in Figure 4.6 and 7, respectively. The pedestrian overpass has the highest peak at the low frequency range due to the potential reason. The pedestrian overpass testing location is open to the air, thereby the sound waves can travel directly from the noise source (such as the AYE) to the measurement point without obstacles to reduce the energy of low-frequency sound waves. Secondly, the elevated position effects will be a potential reason to prove that the pedestrian overpass testing location has the highest peak at low frequency in the spectrum. As the pedestrian overpass is closer to the noise source, the noise might directly come from the vehicle exhaust and the engine, which are significant in the low frequency range as shown in Figure 4.5.

When we compared the result for Figure 4.6 and 7, the peak noise level of the bus station at the 20 Hz frequency is slightly higher than the peak noise level of behind the concrete wall. This potential factors for that because the concrete wall can significantly reduce the transmission of sound energy, especially for low-frequency noise and has a good sound insulation effect.[8]

4.2 Overview of sound experiment at locations on different sides of BLK11 and BLK01

Next, we choose two houses in The Parc Condominium as sound measurement sites. As shown in Figure 4.8 to Figure 4.12, one room is located on the 18th floor of BLK11, facing obliquely towards the AYE at a horizontal distance of approximately 100 metres. The other room is situated on the 14th floor of BLK01 with the bedroom facing West Coast Road and the living room facing West Coast Walk, the former being a normal urban road and the latter a minor road. We measured the data and analyzed it separately for each room, both in the open balcony attached and inside the room with the balcony door either open or closed.

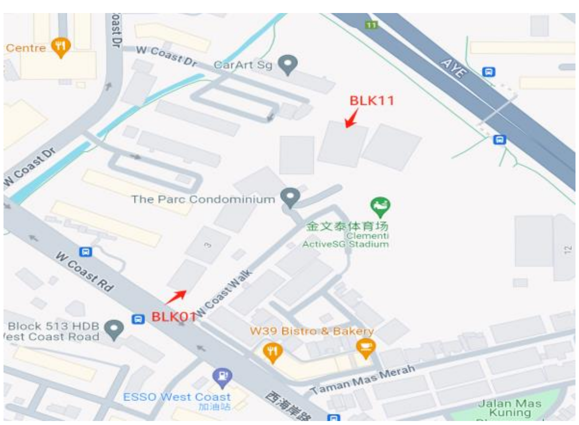

Figure 4.8. Locations of the sound test

Figure 4.9. BLK11-18th floor-Outside the room

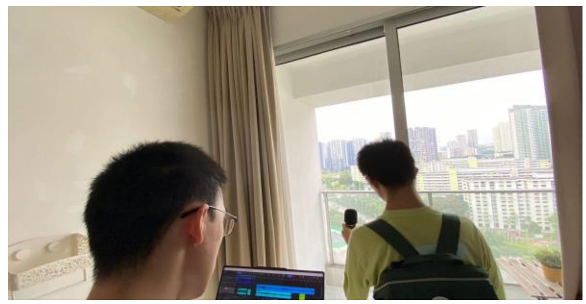

Figure 4.10. BLK11-18th floor-Inside the room-closed door

Figure 4.11. BLK01-14th floor-Inside the bedroom-open door

Figure 4.12. BLK01-14th floor-Outside the living room.

4.2.1 Noise Results at locations

Table 2. Sound measurements-BLK11-18th floor

Measurement location: BLK11-18th floor	Max Sound Level/dB	Min Sound Level/dB	Ave Sound Level/dB
Outside the room	80.5	63.2	66.3
Inside the room-open door	71.7	59.4	62.1
Inside the room-closed door	53.2	45.3	48.9

Table 3. Sound measurements-BLK01-14th floor

Measurement location: BLK01-14th floor	Max Sound Level/dB	Min Sound Level/dB	Ave Sound Level/dB
Outside the bedroom	60.4	55.2	57.1
Inside the bedroom-open door	59.3	53.4	56.2
Inside the bedroom-closed door	56.4	48.7	51.9
Outside the living room	69.5	54.3	59.8
Inside the living room-open door	61.7	50.4	54.2
Inside the living room-closed door	53.3	45.5	49.1

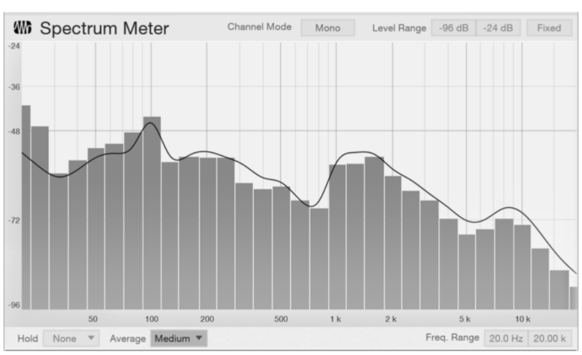

Figure 4.13. Spectrum of BLK11-Outside the room

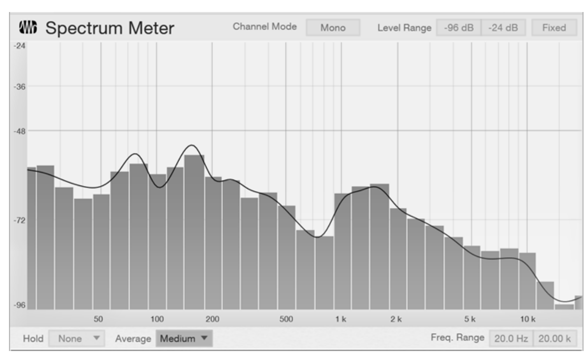

Figure 4.14. Spectrum of BLK11-Inside the room-open door

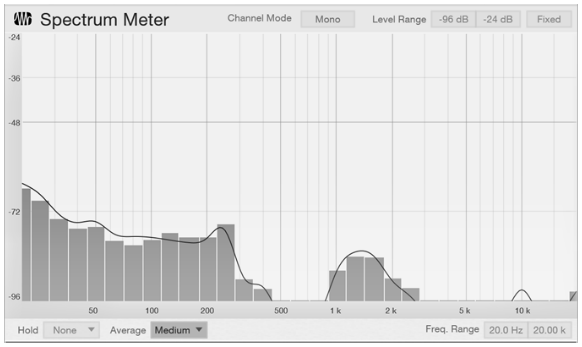

Figure 4.15. Spectrum of BLK11-Inside the room-closed door

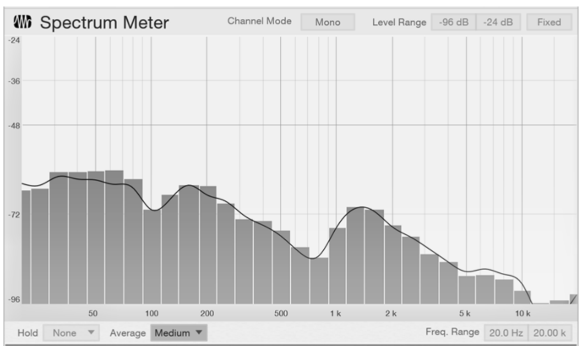

Figure 4.16. Spectrum of BLK01-Outside the bedroom

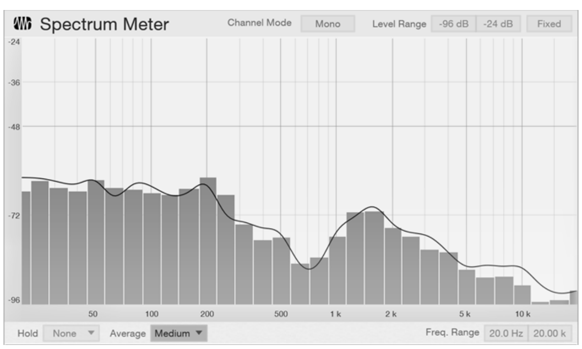

Figure 4.17. Spectrum of BLK01-Inside the bedroom-open door

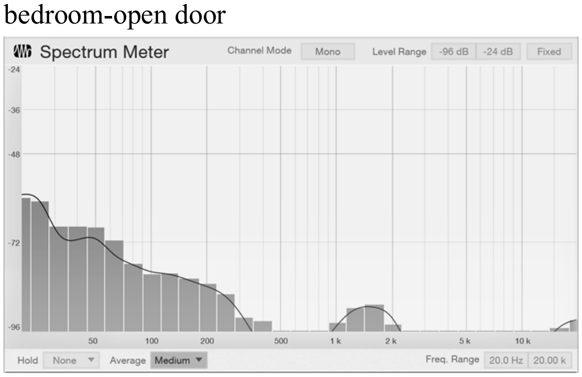

Figure 4.18. Spectrum of BLK01-Inside the bedroom-closed door

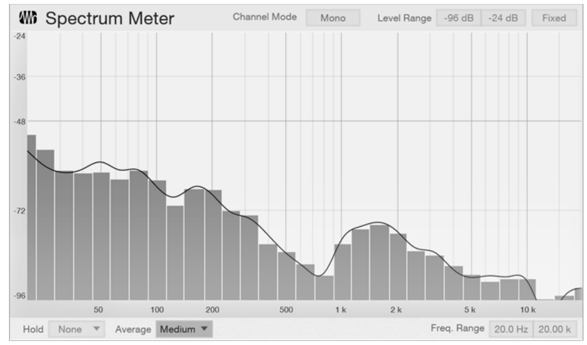

Figure 4.19. Spectrum of BLK01-Outside the living room

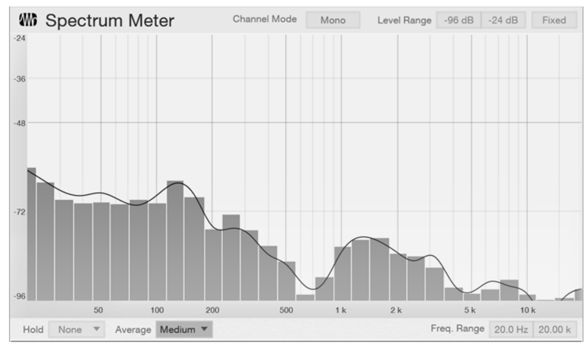

Figure 4.20. Spectrum of BLK01-Inside the living room-open door

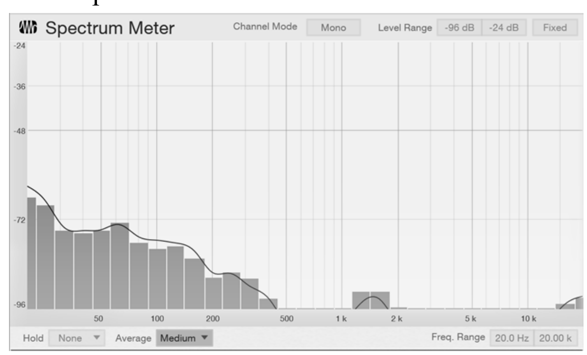

Figure 4.21. Spectrum of BLK01-Inside the living room-closed door

4.2.2 Noise Results Comparison

According to Tables 2 and 3, we obtained the basic sound levels at each measurement point in these rooms. Firstly, in each room, the same pattern exists for the sound level with respect to the location: the sound level outside the room is greater than inside the room with the door open, and inside the room with the door open is greater than inside the room with the door closed. Then we find that the orientation in which these different rooms are located directly affects their sound levels.

Separately, the sound level of the room located in BLK11(take Outside the room for example) is significantly higher than the two rooms located in BLK01 due to its orientation towards AYE, which is mainly due to the fact that highways generate higher sound levels because of the higher traffic flow and higher speeds compared to ordinary urban roads. The difference in sound levels is not significant for the two rooms facing different directions for BLK01. This may be due to the fact that there is no significant difference in the environment as both sides are residential areas with lower traffic volumes on city roads. The sound level at the room-balcony doorway is always lower than that measured at the outside of the balcony, compared to the room door, which has a more pronounced effect on reducing the sound level.

Figure 4.13 to 21 show the spectrum of these location data, respectively. Firstly, it can be noticed that the spectrum of the out-of-room (balcony) and in-room (open door) states have a similar structure. For the room of BLK11, the sounds with frequencies in the range of 100-150 Hz constitute peaks and the amplitudes of the bands are basically higher than in the room of BLK01. This echoes the inference made above. For BLK01's bedroom, it is more evenly distributed between 20 and 200 Hz, while the peak in the living room occurs around 20 Hz. This is related to the different composition of sound in different locations.

In addition, from outside the room to inside the room (with the door open), there is a decrease in the amplitude of the sound level in all frequency bands, with a greater decrease in BLK11, which may be due to the differences in the structure of the balcony and the layout of the neighbourhood in which it is located. The sound insulation after closing the door is much better than in the open door condition. For these rooms, all frequency bands show a significant decrease in amplitude after the door is closed, with most of the mid- and high-frequency bands above 500 Hz dropping to close to 0 dB. The balcony doors in these three rooms are made of glass, so there is a factor of sound attenuation that the glass reflects or absorbs a large amount of sound waves, especially in the mid- and high-frequency bands. The most sensitive band of the human ear is 500-8000Hz, so the body feels quieter in the closed room.

4.3 Overview of sound experiment at locations on different floors of BLK01

In the section of sound experiments conducted on different floors of BLK01, our objective is to evaluate whether the effect of the greenery contributes to the reduction of the urban noise. We examined the noise levels on the 3rd floor as shown in Figure 4.22, which is covered by the greenery, as well as on the 14th in Figure 4.23 and 20th floors in Figure 4.24, where both locations are without greenery.

Figure 4.22. 3rd floor-covered by greenery

Figure 4.23. 14th floor

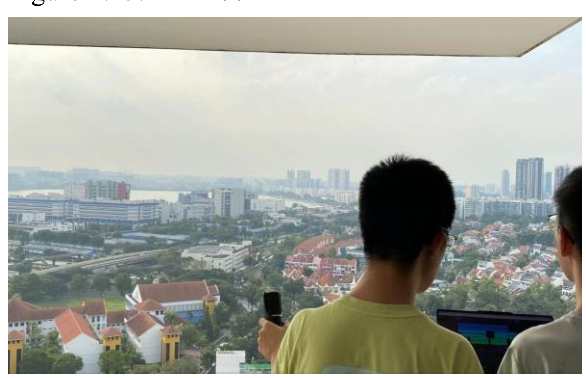

Figure 4.24. 20th floor

4.3.1 Noise Results at locations

Table 4. Sound measurements-BLK01-different floors

Measurement location: BLK01-different floors	Max Sound Level/dB	Min Sound Level/dB	Ave Sound Level/dB
3rd floor-covered by greenery	63.9	48.6	54.3
14th floor	73.2	52.8	57.5
20th floor	65.1	51.7	56.3

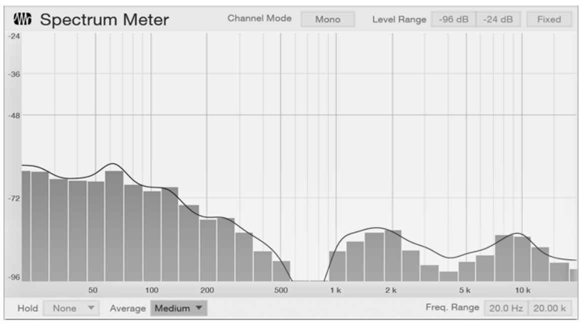

Figure 4.25. Spectrum of outside the 3rd floor covered by greenery

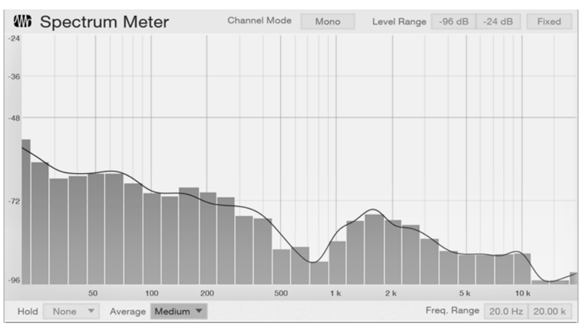

Figure 4.26. Spectrum of outside the 14th floor without greenery

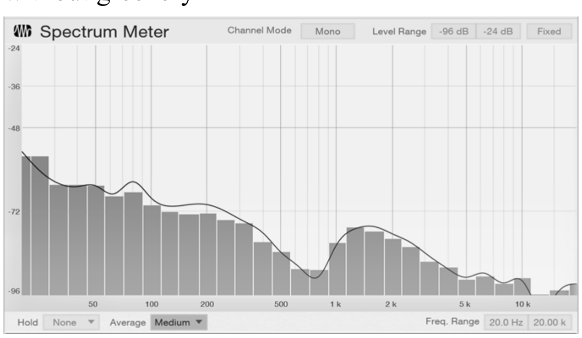

Figure 4.27. Spectrum of outside the 20th floor without greenery

4.3.2 Noise Results Comparison

From Table 4, it can be seen that in general the sound levels measured at higher floors decrease gradually. However, the sound level is lower on the 3rd floor, which is isolated by greenery.

In Figure 4.25, Figure 4.26, and Figure 4.27, the peak of noise level occurs in the low frequency region. Compared to the low frequency range of 20 Hz to 50 Hz, Figure 4.25 for the spectrum outside the 3rd floor with greenery shows the lowest peak noise levels. In this sound experiment, the greenery acts as the noise barriers. According to the Construction Noise - Control and Mitigation power at slide 24, the outdoor noise barriers can effectively reduce the noise level transmitted from the noise source to the receiving point.[9] The underlying reason is the sound absorption function of the greenery, which can absorb sound waves. When the sound passes through the greenery, some of its energy is absorbed by the plant, thus reducing the intensity of the sound transmitted to the other side. On the other hand, the 14th floor and 20th floor exhibit significantly higher peak noise levels than the 3rd floor. According to the Construction Noise - Control and Mitigation power at slide 37, the main reason is that noise barriers are less efficient at higher floors, which are further away from the greenery. [10] As shown in Figure 4.26 and 27, the peak noise levels at low frequencies for high floors are higher than those for lower floors with greenery. It could be assumed that the noise on high floors originates from birds or planes, which affects the noise levels at low frequencies in the spectrum.

4.4 Brief Waterfall Analysis

At the same time, a brief analysis of the changes in the spectrum over time was also carried out, roughly as shown in Figure 4.s 28 to 32.

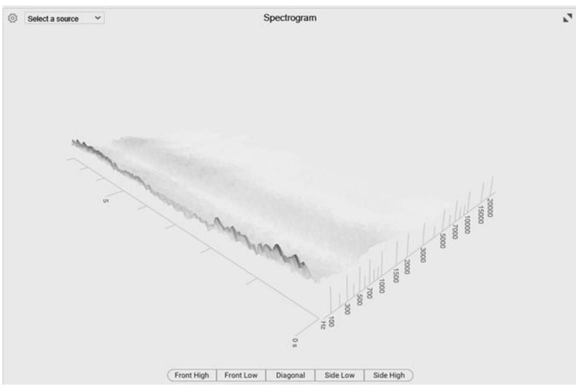

Figure 4.28. On the Pedestrian Overpass

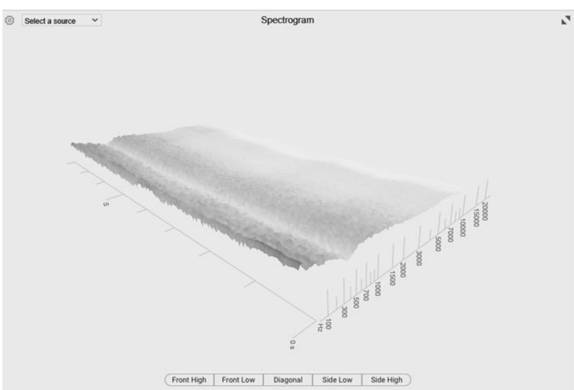

Figure 4.29. BLK11-Outside the room

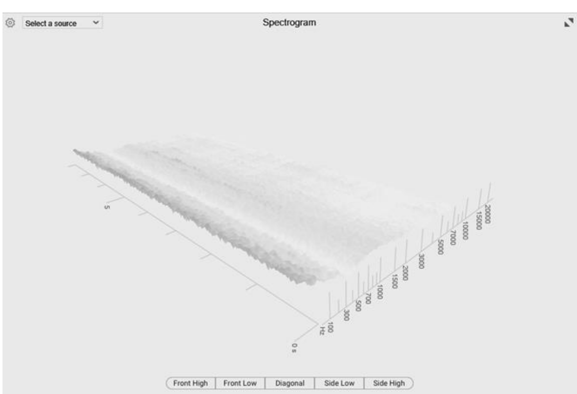

Figure 4.30. BLK01-Inside the bedroom-open door

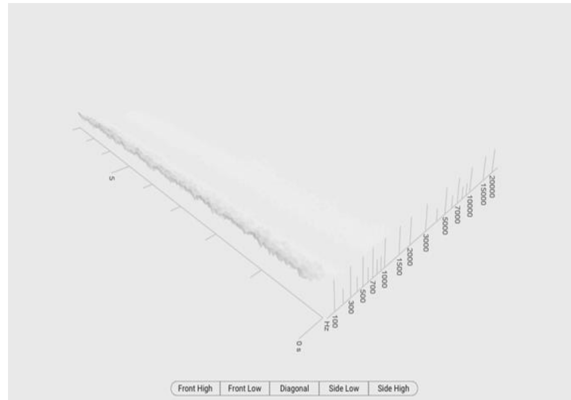

Figure 4.31. BLK01-living room-closed door

For most of the cases we measured, the spectra did not change significantly in their main characteristics over time. The main cases are: as shown in Figure 4.28, there are fluctuations in one frequency band (low frequency), which is due to differences in vehicle types, speeds, etc.; as shown in Figure 4.29, there is a small change in the frequency bands relative to the whole; and as shown in Figure 4.30 and 31, it is relatively stable over time.

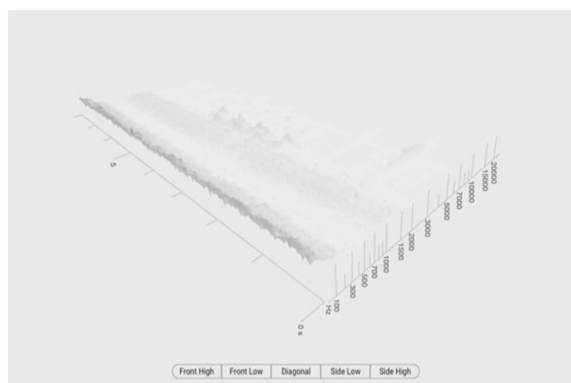

Figure 4.32. BLK01-3rd floor covered by greenery

However, there is also a case where the spectrum changes character at some point due to the influence of individual extraordinary sounds. As shown in Figure 4.32, during the measurement process, peaks with a frequency of 1500-2000 Hz can be observed on the waterfall plot at several points in time because of the high number of birdsongs in the neighbourhood. Combined with the measurement files, the frequency characteristics of some specific sounds can be quickly determined.

5. Conclusion

In conclusion, the result we provided in the data analysis, we conclude that the environment features, such as the location of opening to the air and the height of the location, as well as the physical barrier, such as concrete walls, play a key role in determining the noise level of the locations. Especially in the low frequency region, the influence of these factors on the noise transmission is particularly obvious. Also, the sound insulation of the room is significantly affected by the door closed, the direction of the room where some rooms are direct to the main noise sources, and as well as the structure and layout of the building. The enclosed room provides significant sound attenuation, especially for medium and high frequency noise, which helps to create a quieter living environment. Furthermore, we also can conclude that greenery plays an important role in reducing noise levels. Especially in the low floors, the greening can effectively act as a noise barrier and reduce the noise level. However, as at the higher floor, the soundproofing effect of the greenery diminishes, resulting in relatively high noise levels on the upper floors. This highlights the importance of considering noise control measures in urban planning and architectural design, especially for the design of tall buildings. Last but not least, the waterfall spectrum provides an image to prove that although the main characteristics of ambient noise remain stable most of the time, special sound events, such as birdsong, are still able to cause noticeable changes in the spectrum. This highlights the importance of considering the special sound sources that may be present in the environment when conducting noise assessment and control.

Reference

[1]Howard, D., & Angus, J. (2009). “Acoustics and Psychoacoustics” (4th ed.).

[2] Changqing Xu. “Fourier matrices and Fourier tensors.” Frontiers of Mathematics in China, 2021.

[3] “The Fast Fourier Transform.” Wikipedia, Wikimedia Foundation, 20 Feb. 2024, en.wikipedia.org/wiki/Fast_Fourier_transform

[4] “Insertion loss concepts.” Wikipedia, Wikimedia Foundation, 20 Jul. 2023, en.wikipedia.org/wiki/Insertion_loss

[5] G. D. Bergland, “A guided tour of the fast Fourier transform,” IEEE Spectrum, vol. 6, no. 7, pp. 41-52, 1969.

[6] “Sampling and the Nyquist frequency.”, Wikipedia, Wikimedia Foundation, 18 Mar. 2023, en.wikipedia.org/wiki/Nyquist_frequency.

[7] “Ayer Rajah Expressway.” Wikipedia, Wikimedia Foundation, 17 Dec. 2023, en.wikipedia.org/wiki/Ayer_Rajah_Expressway.

[8] Contacthifi, et al. “Low Frequency Absorbing Materials.” Acoustic Fields, 14 Mar. 2020, www.acousticfields.com/low-frequency-absorbing-materials.

[9] Lee, Heow Pueh. “Construction Noise - Control and Mitigation.” ME5106 Engineering Acousics (Depatment of Mechanical Enginering at National University of Singapore) slide 24. 23 Feb. 2024.

[10] Lee, Heow Pueh. “Construction Noise - Control and Mitigation.” ME5106 Engineering Acousics (Depatment of Mechanical Enginering at National University of Singapore) slide 37. 23 Feb. 2024.